Cyclic Behavior of a Laterally-Loaded Monopile in Spatially Variable London Clay

T.S. Charlton[1] and M. Rouainia[2]

[1]School of Engineering, Newcastle University, UK.
E-mail: t.s.charlton@newcastle.ac.uk
[2]School of Engineering, Newcastle University, UK.
E-mail: mohamed.rouainia@newcastle.ac.uk

Abstract: The performance of monopiles in cohesive soils is of great interest for future offshore wind farm developments, particularly under the cyclic loads that typify the offshore environment. Clay behavior during undrained cyclic loading is complex and involves the accumulation of plastic strains, generation of excess pore water pressures and degradation of initial stiffness. In this paper, the cyclic behavior of a laterally-loaded monopile in spatially variable clay is investigated for the first time. A kinematic hardening constitutive model is used in a 3D finite element analysis to capture the hysteretic stress-strain behavior of the clay. The monopile is installed in overconsolidated London Clay, which is present at several offshore wind farms in the Thames Estuary. The finite element model is coupled with random field representations of initial stiffness and clay structure. The statistical characterization of the random fields was undertaken considering parameter ranges observed in laboratory tests. Under one-way cyclic loading, the monopile showed ratcheting behavior, where pile rotation accumulates with increasing numbers of load cycles. The cyclic secant stiffness also increased with the number of load cycles due to the generation of negative excess pore pressures in the clay. Spatial variability did not affect the observed ratcheting and stiffening behavior but the range in monopile response demonstrates how the natural spatial variability of clay can have a strong influence on monopile performance.

Keywords: Offshore wind; monopile; cyclic; spatial variability; London clay.

1 Introduction

Monopiles have proven to be an effective foundation for offshore wind turbines (OWTs) in waters of up to 35m depth and currently account for 81% of existing OWT foundations in Europe (Wind Europe 2017). The offshore environment subjects monopiles to a high number of load cycles during its lifetime. This cyclic loading can lead to permanent displacement and rotation of the pile. To maintain safe operation of the OWT, the monopile must be designed so that the rotation does not exceed a serviceability limit, for example 0.5° (Achmus et al. 2009). The majority of research into the cyclic behavior of monopiles has focused on monopiles in sand (Achmus et al. 2009; LeBlanc et al. 2010; Barari et al. 2017) but monopile behavior in clay will become increasingly important due to the worldwide growth of offshore wind. In clay, centrifuge tests have been carried out by Zhang et al. (2011) and Lau (2015). Both studies showed that monopile behavior in clay involves the complex interplay of a variety of physical phenomena, including remolding of the clay and the generation of excess pore water pressures.

In addition to the lack of detailed understanding of the cyclic behavior of laterally-loaded monopiles in clay, it is important to remember that real site conditions are also highly variable. Le et al. (2014) recently reported a case study of the Sheringham Shoal wind farm, characterized by two heavily overconsolidated clay strata (Bolders Bank and Swarte Bank formations) interbedded with a layer of dense sand. Both the undrained shear strength (s_u) and small-strain stiffness of the clay layers showed considerable variability, and the degradation of initial stiffness under monotonic and cyclic loading was an important factor in design. Haldar and Sivakumar Babu (2008) considered the effect of 2D spatial variability on the ultimate lateral capacity of a monopile in clay. However, the effect on cyclic behavior has received little attention. Depina et al. (2015) coupled the degradation stiffness model with a random field of stiffness to investigate the influence of spatial variability on cyclic performance of a monopile in dense sand. It was found that spatial variability could affect the accumulated displacement and rotation of the pile considerably.

In this paper, the cyclic behavior of a laterally-loaded monopile in spatially variable London Clay will be investigated using 3D finite element (FE) analysis. A kinematic hardening constitutive model is used to capture the hysteretic stress-strain behavior of the clay under cyclic loading. Spatial variability is represented by random fields and the effect on monopile performance under cyclic loading is quantified by Monte Carlo simulation.

2 Constitutive Model for London Clay

London Clay is a stiff, overconsolidated clay with behavior characterised by a natural structure that has the effect of increasing peak strength (Gasparre et al. 2007). In the context of monopile foundations, London Clay holds

Proceedings of the 7th International Symposium on Geotechnical Safety and Risk (ISGSR)
Editors: Jianye Ching, Dian-Qing Li and Jie Zhang

Published by Research Publishing, Singapore.
ISBN: 978-981-11-2725-0; doi:10.3850/978-981-11-2725-0_IS9-1-cd

interest as it is present in the Thames Estuary where the London Array and Kentish Flats wind farms are located. The Kinematic Hardening Structure Model (Rouainia and Muir Wood 2000) is a multi-surface effective stress model based on the critical state framework. The KHSM extends the classic Modified Cam Clay (MCC) model by including an outer structure surface that collapses towards the MCC reference surface, which describes the behavior of fully remoulded clay, and a kinematic hardening bubble that moves inside the structure surface and encloses the elastic domain. The influence of structure is controlled through the parameter r, which represents the ratio of the size of the structure surface to the size of the reference surface ($r > 1$). The formulation is apt for simulating both the natural structure of London Clay and the hysteretic stress-strain behavior under dynamic or cyclic loads.

The degradation of stiffness is captured through a bounding surface relationship, with stiffness dependent on the distance between the bubble and structure surface. The initial stiffness, G_0, is described using a nonlinear elastic formulation by Viggiani and Atkinson (1995):

$$\frac{G_0}{p'_r} = A_g \left(\frac{p'}{p'_r}\right)^{n_g} {R_0}^{m_g} \tag{1}$$

where p' is the mean effective pressure with a reference value (p'_r) of 1kPa, R_0 is the isotropic overconsolidation ratio ($R_0 = 2P_c/p'$ with P_c the centre of the reference surface) and A_g, n_g and m_g are dimensionless stiffness parameters.

The KHSM parameters were calibrated for London Clay by Gonzàlez et al. (2012). The lithological unit B2(a) has been considered in this study and the model parameters are given in **Table 1**. The overconsolidation ratio was calibrated as 4.5. The clay has a bulk unit weight of 19kN/m^3 and a critical state friction angle of 22°; K_0 is taken as 1.0. In this paper, both the initial degree of structure (r_0) and the small-strain stiffness (A_g) are modelled as random fields to investigate the effect of variability in strength and stiffness on the performance of a monopile under lateral cyclic loading.

Table 1. Calibrated KHSM parameters for London Clay. Shading indicates random parameters in the current study.

Material property	Value
Slope of normal compression line, λ^*	0.0965
Slope of swelling line, κ^*	0.0459
Poisson's ratio, ν	0.3
Critical state stress ratio, M	0.85
Ratio of size of bubble and reference surface, R	0.016
Stiffness interpolation parameter, B	4.0
Stiffness interpolation exponent, ψ	6.0
Initial degree of structure, r_0	2.5 (μ_{r_0})
Destructuration strain parameter, A	0.75
Destructuration parameter, k	1.0
Non-dimensional stiffness parameter, A_g	430 (μ_{A_g})
Non-dimensional stiffness parameter, n_g	0.87
Non-dimensional stiffness parameter, m_g	0.28

3 Variability of London Clay

3.1 Clay structure

Considerable natural variability in undrained shear strength is a commonly observed feature of London Clay (Hight et al. 2003). Stress-strain behavior in undrained triaxial tests on samples from a range of lithological units have shown similar characteristics, namely strain-softening and dilatant behavior (Gasparre et al. 2007). Differences in peak strength are a result of variation in cementing, density and plasticity index in addition to fissures and discontinuities (Gonzàlez et al. 2012). Using the KHSM, this variability can be captured through the degree of structure. Figure 1 shows numerical and laboratory results of undrained triaxial compression tests on London Clay. A higher r_0 results in a higher peak strength while the strain-softening behavior remains. Each numerical prediction tends to the same remolded strength at large strains as the parameters controlling the reference surface are unchanged. The calibrated value of r_0 fits the experimental data satisfactorily but the figure shows how the clay response can vary.

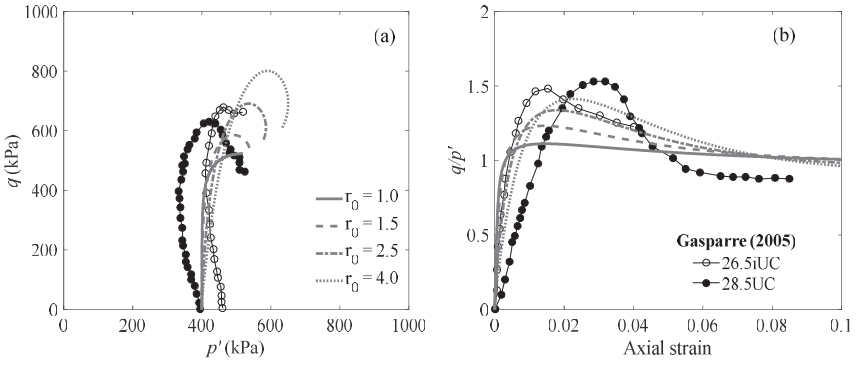

Figure 1. KHSM predictions and laboratory data for undrained triaxial compression tests on London Clay: (a) stress path; (b) stress-strain response.

The statistics of r_0 are based on those of s_u, which is generally assumed to follow a lognormal distribution (Lacasse and Nadim 1996; Phoon and Kulhawy 1999). A shifted lognormal distribution is assumed for r_0, with a lower bound equal to 1. The coefficient of variation (COV) of r_0 is chosen to be 0.3 in the present study, based on the typical range of variability of s_u reported in the literature. The COV is a slightly lower value than found by Le et al. (2014) at Sheringham Shoal for several clay layers (COV = 0.49-0.6), but only a limited number of tests were available there. A square exponential autocorrelation function is assumed and the autocorrelation distances in horizontal and vertical directions are taken to be 10m and 1m respectively, which is characteristic of many soil parameters (Phoon and Kulhawy 1999).

3.2 Small-strain stiffness

The small-strain stiffness behavior of London Clay has been characterized in studies by Hight et al. (2003) and Hight et al. (2007). The data is summarized in Figure 2 in terms of the undrained secant elastic modulus $E_{u,sec}$. The experimental bounds show that at very small strains (10^{-5} to 10^{-4}), a large range of stiffness values were recorded, indicating the uncertainty associated with the initial stiffness. The variability of small-strain stiffness and its degradation with strain is represented by modelling the KHSM parameter A_g as a random field. A lognormal distribution is chosen to ensure A_g takes positive values. The COV of A_g and G_0 are equivalent by way of Eq. (1); COV_{A_g} is therefore taken as 0.4, which fits into the range identified at Sheringham Shoal, where COV_{G_0}= 0.37-0.67.

To model the dependency between structure and small-strain stiffness (e.g. Cafaro and Cotecchia 2001), the random field of A_g is assumed to have the same autocorrelation structure as r_0 and the two fields are assigned a strong positive cross-correlation of $\rho_{r_0 A_g}$= 0.8.

3.3 Random field generation

The lognormal distribution is parametrized by α and β, respectively the mean and standard deviation of the logarithm of the random variable. The shifted lognormal distribution has an additional parameter, δ, to specify the lower bound. The random fields of r_0 and A_g are therefore generated as follows:

$$r_0(x,y,z) = \delta_{r_0} + \exp\left(\alpha_{r_0} + \beta_{r_0} G_{r_0}(x,y,z)\right) \tag{2}$$

$$A_g(x,y,z) = \exp\left(\alpha_{A_g} + \beta_{A_g} G_{A_g}(x,y,z)\right) \tag{3}$$

where G_{r_0} and G_{A_g} are correlated standard Gaussian random fields of zero mean and unit variance. A series expansion method (Li and Der Kiureghian 1993) is used to simulate the random fields, which are cross-correlated following Vořechovský (2008). The random field values are subsequently mapped onto the integration points of the FE model.

4 Finite Element Model

A 3D FE model (Plaxis 2016) is used, based on centrifuge tests carried out by Lau (2015) where a monopile with a diameter of 3.8m and an embedded length of 20m (in prototype scale) was considered. The FE mesh, consisting of 10-node tetrahedral elements, is shown in Figure 3. To reduce computational time, only half the pile is modelled. The monopile is represented by a block of linear elastic material. Soil-structure interaction is

modelled through interface elements with a reduced strength of φ' = 14°. Viscous lateral boundaries are used to absorb outgoing energy in dynamic analyses and undrained conditions apply.

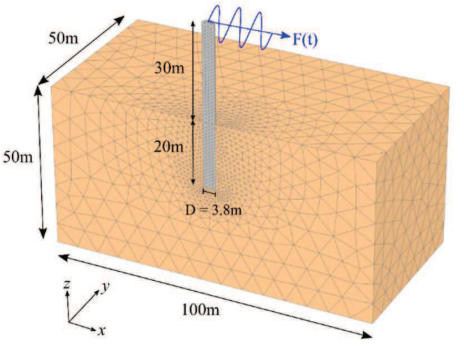

Figure 2. Finite element mesh.

The characteristics of the cyclic loading can be described by two parameters, ζ_b and ζ_c. The parameters are defined in terms of the applied force as $\zeta_b = F_{max}/F_R$ and $\zeta_c = F_{min}/F_{max}$, where F_R is the static capacity (4.66MN) and F_{max} and F_{min} are the maximum and minimum load applied in each cycle, respectively. Here, one-way load cycles are considered ($\zeta_c = 0$) with the load magnitude representative of loading at the fatigue limit state ($\zeta_b = 0.18$) (LeBlanc et al. 2010). The loads are applied through a dynamic sinusoidal force with a frequency of 0.2Hz, imposed at the top of the pile.

5 Results and Discussion

For this paper, 100 Monte Carlo simulations are used to characterize the monopile response. Due to the computational demands, the number of applied load cycles is limited to 50 for each simulation. Example random field realizations are shown in Figure 3.

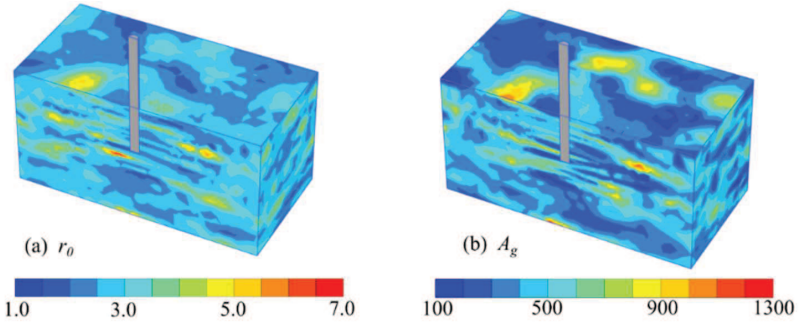

Figure 3. Random field realisations of (a) r_0 and (b) A_g.

Figure 4 shows the bending moment-rotation behavior at the mudline. For the deterministic analysis, both r_0 and A_g are equal to their mean values with clay structure and small strain stiffness homogeneous across the soil domain. In the first cycle, the pile rotation does not return to zero as the load is released due to the development of plastic strain during the load cycle. Instead, nonlinear hysteresis loops form. The hysteresis loops do not close, meaning that with continuing cycles of loading-unloading the pile experiences increasing rotation, or ratcheting. It can be seen that the general behavior in spatially variable clay follows that observed in the deterministic analysis, with hysteresis loops forming that tighten with increasing numbers of load cycles. However, the rotation that occurs in each cycle can vary due to the changing spatial distribution of small-strain stiffness and clay structure around the monopile. After only 50 load cycles, the difference in accumulated rotation can be as great as 10%.

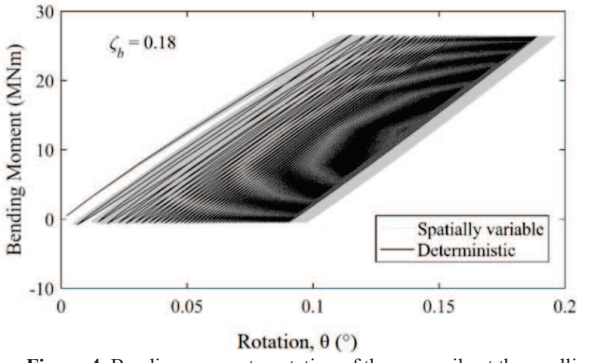

Figure 4. Bending moment - rotation of the monopile at the mudline.

The accumulated rotation can be normalized as $\Delta\theta_N / \theta_1$, where $\Delta\theta_N = \theta_N - \theta_1$, θ_1 is the maximum rotation in the first cycle rotation and θ_N is the maximum rotation in cycle N. The normalized accumulated rotation is plotted in Figure 5, with the normalizing factor θ_1 updated for each simulation. The rate of rotation accumulation consistently decreases in each cycle in an attenuation mechanism. It is clear that the spatial variability of the clay does not affect the trend of attenuation of the accumulated rotation with the number of load cycles.

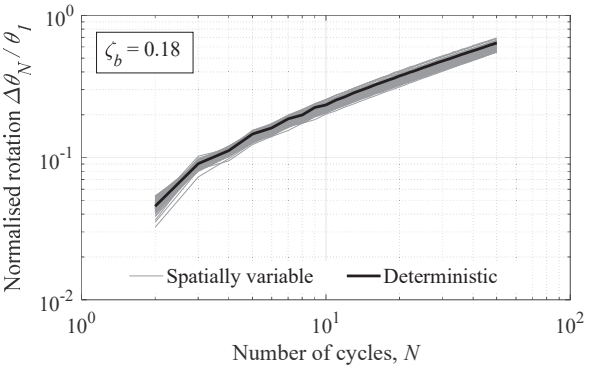

Figure 5. Normalised accumulated rotation at the mudline in spatially variable clay.

The cyclic secant stiffness is presented in Figure 6(a) and can be seen to increase with the number of load cycles. Similar to the accumulated rotation, a rapid increase in secant stiffness occurs during the first few cycles but the rate of increase reduces in each cycle. An increase in foundation stiffness would lead to an increase in the natural frequency of the OWT-foundation system, which is an important design consideration. In spatially variable clay, there is initially a wide range in secant stiffness. As evident in Figure 6(b), the COV of k_c reduces with the number of cycles. The stiffening behavior is a result of the generation of negative excess pore water pressure in the overconsolidated clay around the monopile as it is subjected to repeated load cycles. Despite the degradation of the initial clay stiffness with plastic strain, the overall stiffness of the foundation increases.

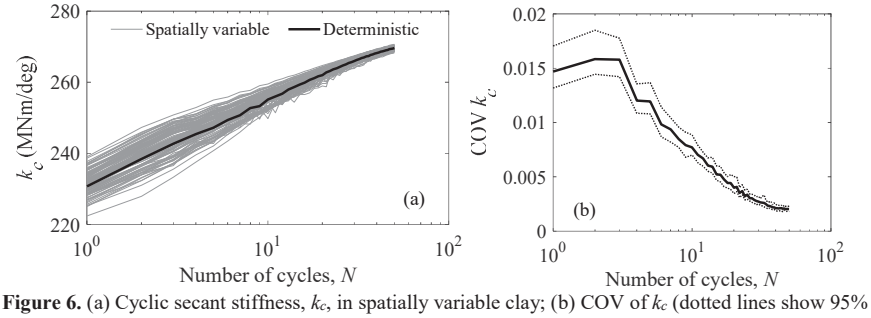

Figure 6. (a) Cyclic secant stiffness, k_c, in spatially variable clay; (b) COV of k_c (dotted lines show 95% CI).

6 Conclusions

A study of monopile performance under lateral cyclic loading in spatially variable London Clay has been undertaken using 3D FE analysis. The clay was simulated using a kinematic hardening constitutive model. Under one-way cyclic loading, the monopile exhibited ratcheting behavior where rotation accumulates with increasing numbers of load cycles. The cyclic secant stiffness also increased, although it is unclear whether this would continue beyond the number of cycles considered in this study. These trends are related to the generation of negative excess pore water pressures around the monopile, which occurred due to the overconsolidated state of the clay. Spatial variability of stiffness and clay structure can have a significant effect on monopile rotation and the overall stiffness of the foundation system. For example, after only 50 load cycles the accumulated rotation could be as much as 10% greater than the deterministic prediction.

Acknowledgments

The first author would like to thank the Engineering and Physical Sciences Research Council (EPSRC) and Atkins for funding this research.

References

Achmus, M., Kuo, Y., and Abdel-Rahman, K. (2009). Behavior of monopile foundations under cyclic lateral load. *Computers and Geotechnics*, 36(5), 725-735.

Barari, A., Bagheri, M., Rouainia, M., and Ibsen, L.B. (2017). Deformation mechanisms for offshore monopile foundations accounting for cyclic mobility effects. *Soil Dynamics and Earthquake Engineering*, 97, 439-453.

Cafaro, F. and Cotecchia, F. (2001). Structure degradation and changes in the mechanical behaviour of a stiff clay due to weathering. *Géotechnique*, 51(5), 441-453.

Depina, I., Le, T.M.H., Eiksund, G., and Benz, T. (2015). Behavior of cyclically loaded monopile foundations for offshore wind turbines in heterogeneous sands. *Computers and Geotechnics*, 65, 266-277.

Gasparre, A., Nishimura, S., Coop, M.R., and Jardine, R.J. (2007). The influence of structure on the behaviour of London Clay. *Géotechnique*, 57(1), 19-31.

Gonzàlez, N.A., Rouainia, M., Arroyo, M., and Gens, A. (2012). Analysis of tunnel excavation in London Clay incorporating soil structure. *Géotechnique*, 62(12), 1095-1109.

Haldar, S. and Sivakumar Babu, G.L. (2008). Effect of soil spatial variability on the response of laterally loaded pile in undrained clay. *Computers and Geotechnics*, 35(4), 537-547.

Hight, D.W., Gasparre, A., Nishimura, S., Minh, N.A., Jardine, R.J., and Coop, M.R. (2007). Characteristics of the London Clay from the Terminal 5 site at Heathrow Airport. *Géotechnique*, 57(1), 3-18.

Hight, D.W., McMillan, F., Powell, J.J.M., Jardine, R.J., and Allenou, C.P. (2003). Some characteristics of London Clay. In Tan, T.S., Phoon, K.K., Hight, D.W., and Leroueil, S. (eds.). *Characterisation and Engineering Properties of Natural Soils*, Lisse, NL: Balkema, 851-907.

Li, C. and Der Kiureghian, A. (1993). Optimal discretization of random fields. *Journal of Engineering Mechanics*, 119(6), 1136-1154.

Lacasse, S. and Nadim, F. (1996). Uncertainties in characterising soil properties. *Uncertainty in the Geologic Environment:Ffrom Theory to Practice,* New York: ASCE, 49-75.

Lau, B.H. (2015). *Cyclic Behaviour of Monopile Foundations for Offshore Wind Turbines in Clay.* PhD Thesis, University of Cambridge.

Le, T.M.H., Eiksund, G.R., Strøm, P.J., and Saue, M. (2014). Geological and geotechnical characterisation for offshore wind turbine foundations: A case study of the Sheringham Shoal wind farm. *Engineering Geology*, 177, 40-53.

LeBlanc, C., Houlsby, G.T., and Byrne, B.W. (2010). Response of stiff piles in sand to long-term cyclic lateral loading. *Géotechnique*, 60(2), 79-90.

Phoon, K.K. and Kulhawy, F.H. (1999). Characterization of geotechnical variability. *Canadian Geotechnical Journal*, 36(4), 612-624.

Plaxis (2016). *PLAXIS 3D AE* - Reference Manual. Delft: Plaxis BV.

Rouainia, M. and Muir Wood, D. (2000). A kinematic hardening constitutive model for natural clays with loss of structure. *Géotechnique*, 50(2), 153-164.

Viggiani, G.M.B. and Atkinson, J.H. (1995). Stiffness of fine-grained soil at very small strains. *Géotechnique*, 45(2), 249-265.

Vořechovský, M. (2008). Simulation of simply cross correlated random fields by series expansion methods. *Structural Safety*, 30(4), 337-363.

Wind Europe (2017). *The European Offshore Wind Industry: Key Trends and Statistics 2016*. Brussels: Wind Europe.

Zhang, C., White, D., and Randolph, M. (2011). Centrifuge modeling of the cyclic lateral response of a rigid pile in soft clay. *Journal of Geotechnical and Geoenvironmental Engineering*, 137(7), 717-729.